Available online at www.sciencedirect.com

ScienceDirect

Procedia Technology 22 (2016) 78 – 85

Procedia Technology

9th International Conference Interdisciplinarity in Engineering, INTER-ENG 2015, 8-9 October 2015, Tirgu-Mures, Romania

Application of the Inverse Finite Element Approach for the Fast Simulation of Tube Hydroforming

Mohamed-Saïd Chebbah[a,]*, Nacer Hebbir[a], Toufik Kanit[b], Sara Dehimi[c]

[a]*Departmentof Mechanical Engineering, University Mohamed Khider of Biskra, Po.Box 145 - 07000, Algeria*
[b] *Laboratoire de Mécanique de Lille, LML, CNRS/UMR 8107, 59655 Villeneuve d'Ascq, France*
[c] *Ecole Normale Supérieure de Kouba, B.P N°92 16308 Vieux-Kouba – Alger, Algérie*

Abstract

In this paper we present an inverse finite element approach for the simulation of anisotropic tube hydroforming operation. This method exploits the knowledge of the final part shape, by starting from this later we search for the nodal positions in the initial cylindrical tube which verify the equilibrium of the final part. We propose a geometrical initial solution allows avoiding the problem of vertical walls and reverse taper. Two numerical applications concerning the hydroforming of T and Y-shaped tubes made from welded low carbon steel AISI 1008-galvanized, using the flow stress data obtained from bulge test have been utilized to validate the method. Verifications of the obtained results have been carried out using the classical explicit dynamic incremental approach (EDIA) by ABAQUS® commercial code to show the efficiency of our approach.

Peer-review under responsibility of the "Petru Maior" University of Tirgu Mures, Faculty of Engineering

Keywords: Inverse approach;large elastoplastic strains; shell element;T-shaped tube; Y-shaped tube.

1. Introduction

Hydroforming is one of the important processes used to shape ductile metals, this technology uses hydraulic pressure to form tube and sheet materials into desired shapes inside die cavities. The preliminary design of forming

* Corresponding author. Tel.: +213-6-6838-5925.
E-mail address: ms.chebbah@univ-biskra.dz

Peer-review under responsibility of the "Petru Maior" University of Tirgu Mures, Faculty of Engineering
doi:10.1016/j.protcy.2016.01.013

processes implies expensive trials-and-errors on forming tools. The use of the numerical simulations is become indispensable to predict the forming feasibility and to optimize the process parameters and the tool geometry [1].

Generally for the simulation of metal forming process there are two approaches: the incremental approach and the inverse approach (IA). By the first one the physical phenomena is simulated step by step, which makes it practically accurate but very time-consuming. On the contrary, the IA allows the fast modeling in only one step, avoiding the contact treatment and the incremental plastic integration. This method is used initially to simulate the stamping and deep drawing process, for example we can cite the work of Guo et al. [2] and Liu and Karima [3]. An extension of this kind of method has been done in order to treat the modeling and simulation of the tube hydroforming. Based on our knowledge a few works have been done on this subject.

In a simple application limited to the round tubes, Nguyen et al. [4] used the IA to analyze cylindrical tube hydroforming, where the final configuration is axisymmetric. Fu et al. [5] proposed a study on one-step simulation for the bending process of extruded profiles. Chebbah et al. [6] proposed a specific methodology based on the coupling between the IA and a Response Surface Method based on diffuse approximation using an axisymmetric membrane/bending shell element. In another works the authors Chebbah et al. [7] introduce new enhancements to their algorithm in order to deal with hydroforming of tubes of general shapes (the initial tube is still cylindrical). More recently, Einolghozati et al. [8] applied an inverse finite element method to predict the main parameters in tube hydroforming process (The initial length of tube or axial feeding, the strain distribution and fluid pressure by employing the equilibrium equations and the flow rule).

In this paper, we propose a geometrical initial solution allows avoiding the problem of vertical walls and reverse taper. Two numerical applications concerning the hydroforming of T-shaped and Y-shaped tubes made from welded low carbon steel AISI 1008-galvanized, using the flow stress data obtained from bulge test [9], have been utilized to validate the method. Verifications of the obtained results have been carried out using the classical EDIA by ABAQUS® commercial code [12] to show the efficiency of our approach.

Nomenclature

∘	initial
δ	virtual
h	thickness
P	intensity of pressure
p,q	point on the mid-surface, in distance z
s	curvilinear coordinate
z	distance of point to the mid surface
u, v, w	displacements in local coordinate
U, V, W	displacements in global coordinate
$\boldsymbol{u_p}$	displacements of p
$\boldsymbol{x}$, $\boldsymbol{dx}$	position vector, its variation
$\boldsymbol{n}$, $\boldsymbol{t}$	normal and tangent vectors in the mid surface
$\boldsymbol{N}$, $\boldsymbol{M}$	membrane forces, bending moments
$\boldsymbol{F_{int}}$, $\boldsymbol{F_{ext}}$	internal and external forces in global coordinate
$\mathbf{B_m}$, $\mathbf{B_f}$	membrane strain, bending strain
$\mathbf{K_t}$	tangent matrix
T	transformation local-global matrix

Greek symbols

r, φ, Z	cylindrical coordinate
λ_1, λ_2, λ_3	principal stretches
$\boldsymbol{\chi}$, $\boldsymbol{e}$	curvature, membrane strains
$\boldsymbol{\varepsilon}$, $\overline{\varepsilon}$	strain, equivalent strain
$\boldsymbol{\sigma}$, $\overline{\sigma}$	stress, equivalent stress

2. Inverse approach for tube hydroforming

The IA is based on the general assumption of knowledge of the final geometry of the 3D part and the total deformation theory of plasticity. The unknowns are material positions of nodes on the initial geometry as well as strains and thickness variations on the final configuration. The strains and stresses are calculated by directly

comparing the initial and final configurations. In the following sections we will present the main stages of the method.

2.1. Initial geometric solution

The inverse method is an iterative method that uses the Newton-Raphson algorithm (NRA) to reach the final solution. Therefore it requires an initial solution. The initial guess representing the guessed nodal positions allows starting the NRA to estimate the strains. To explain the basic concept of the initial solution, the geometric mapping method is described for the hydroforming of cylindrical tubes. The final mid-surface is discretized into triangular shell elements and mapped onto the initial cylindrical tube surface (Fig. 1(a)). Knowing the positions of the element nodes in the final configuration, the first guess can be achieved by the intersection between the projections of the nodes onto the origin (point O in Fig. 1(a)) and the initial cylindrical tube. These positions will be modified iteratively to meet the equilibrium in the final workpiece. This way of projection allows avoiding the superposition of nodes or the reversal of elements may be result from the orthogonal projection (case of vertical walls and reverse taper).

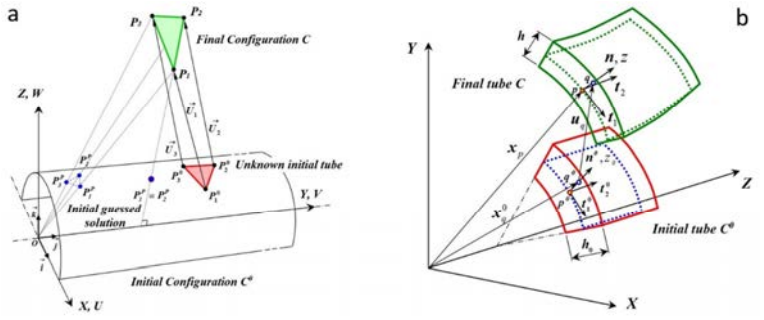

Fig. 1. (a) 3D mesh mapping onto the initial cylindrical tube surface; (b) 3D shell kinematics in tube hydroforming.

2.2. Large Strain Measurement

In the inverse approach only the configurations of the initial tube of cylindrical form C^0 and the final 3D workpiece C are considered. A Kirchhoff assumption has been considered to define the position vectors of material points at the initial and final configuration (Fig. 1(b)). The deformation gradient tensors at points q^0 and q with respect to p are defined in the local coordinate system by:

$$\boldsymbol{dx}_q^0 = \mathbf{F}_0^{-1}\boldsymbol{dx} = \left[\boldsymbol{x}_{p,x} - \boldsymbol{u}_{p,x};\quad \boldsymbol{x}_{p,y} - \boldsymbol{u}_{p,y};\quad \boldsymbol{n}^0 / \lambda_3\right]\boldsymbol{dx} \tag{1}$$

$$\boldsymbol{dx}_q = \mathbf{F}_z^{-1}\boldsymbol{dx} = \left[\boldsymbol{x}_{p,x} + z\boldsymbol{n}_{,x};\quad \boldsymbol{x}_{p,y} + z\boldsymbol{n}_{,y};\quad \boldsymbol{n}\right]\boldsymbol{dx} \tag{2}$$

Where $\boldsymbol{x}= (x, y, z)$ is the position vector at the mid-surface, $\lambda_3=z/z_0=h/h_0$ is the thickness stretch.

The deformation gradient inverse tensor describing the movement between positions q^0 and q referenced in C as follows:

$$\boldsymbol{dx}_q^0 = \mathbf{F}^{-1}\boldsymbol{dx}_q \tag{3}$$

Then, the inverse of the Cauchy–Green left tensor between q and q^0 takes the following form:

$$\mathbf{B}^{-1} = \mathbf{F}^{-\mathrm{T}}\mathbf{F}^{-1} \tag{4}$$

Eigenvalues of the left Cauchy-Green tensor give two principal plane stretches λ_1, λ_2 and their direction transformation matrix **M**. Then, the thickness stretch λ_3 is calculated by the incompressibility assumption.

Finally, the logarithmic strains tensor is obtained as:

$$\boldsymbol{\varepsilon} = \mathbf{M}\ \left[\ln \lambda\right]\ \mathbf{M}^{\mathrm{T}} \tag{5}$$

2.3. Stress computation

In the present IA the elasto-plastic deformation is assumed to be independent of the loading path. The constitutive relations remain in the framework of the deformation theory of plasticity in which Hill's anisotropic criterion is employed to describe the plastic flow. A planar anisotropic sheet is considered. The total constitutive relations can be written by:

$$\boldsymbol{\sigma} = (\mathbf{H}_e^{-1} + (\bar{\sigma} / \bar{\varepsilon}_{\mathrm{p}})\mathbf{P})^{-1}\boldsymbol{\varepsilon} \tag{6}$$

Where $\boldsymbol{\varepsilon}$ is the total strain vector, $\mathbf{H}_{\mathrm{e}}$ is Hooke's elastic constitutive matrix, $\bar{\sigma}$ is the equivalent yield stress, **P** is the matrix defined by the Hill anisotropic criterion, and $\bar{\varepsilon}_p$ is the equivalent plastic strain.

2.4. Equilibrium relationships and 3D shell element used

The principal of virtual work express on the known final 3D configuration leads to:

$$\mathrm{W} = \sum_{\mathrm{elt}} (\mathrm{W}_{\mathrm{int}}^{\mathrm{e}} - \mathrm{W}_{\mathrm{ext}}^{\mathrm{e}}) = 0 \tag{7}$$

Where $\mathrm{W}_{\mathrm{int}}^{\mathrm{e}}$ is the internal virtual work and $\mathrm{W}_{\mathrm{ext}}^{\mathrm{e}}$ is the external virtual work related to the tool actions.

$$\mathrm{W}_{\mathrm{int}}^{\mathrm{e}} = \boldsymbol{\delta U}_n\, \boldsymbol{F}_{\boldsymbol{int}}^{\boldsymbol{e}} \ ;\ \boldsymbol{\delta U}_{\mathrm{n}} = < \delta \mathrm{U}_{\mathrm{i}}\ \delta \mathrm{V}_{\mathrm{i}}\ \delta \mathrm{W}_{\mathrm{i}} > \tag{8}$$

In this work the known 3D configuration is discretized by flat triangular shell elements called DKT12. This element is obtained by assembly of the element of membrane CST (u, v at corner nodes) with the discrete Kirchhoff triangular plate element DKT6 (w at corner nodes and θ_{s} at mid-side nodes). The details formulation of these elements can be obtained from the book of Batoz et al. [10].

In this case the global components of the internal force vector can be defined as:

$$\boldsymbol{F}_{\boldsymbol{int}}^{\boldsymbol{e}} = \mathbf{T}^{\mathrm{T}}(\mathbf{B}_{\mathrm{m}}^{\mathrm{T}}\boldsymbol{N} + \mathbf{B}_{\mathrm{f}}^{\mathrm{T}}\boldsymbol{M})A \tag{9}$$

T is the transformation local-global matrix, $\mathbf{B}_{\mathrm{m}}$ and $\mathbf{B}_{\mathrm{f}}$ are membrane and bending strain respectively and ***N*** and ***M*** are the membrane forces and bending moments respectively.

In the case of no friction, the element external forces due to the hydraulic pressure can be computed using the equilibrium conditions.

$$\boldsymbol{F}_{ext} = \boldsymbol{F}_{\mathrm{int}} = \mathrm{P}\ \boldsymbol{n} \tag{10}$$

Where $\boldsymbol{n}$ is the nodal unit normal vector to the tube, P is the unknown force intensity.

In fact, there are three unknowns at each node (U, V and W) in Cartesian coordinate. Because the radial displacement U_r at every point is known (see Fig. 2), working in a cylindrical coordinate system allows us to reduce the number of unknown displacements for each node to two: circumferential and axial ones (Δφ and W).

At each iteration, the estimation of displacement increment is obtained by the resolution of the following equilibrium equations:

$$\mathbf{K}_t^i \, \Delta \boldsymbol{U} = \boldsymbol{F}_{ext}(\boldsymbol{U}^i) - \boldsymbol{F}_{int}(\boldsymbol{U}^i) = -\boldsymbol{R}(\boldsymbol{U}^i) \tag{11}$$

Where: $\mathbf{K}_t^i = \left[\partial \boldsymbol{R}^i(\boldsymbol{U}) / \partial \boldsymbol{U} \right]$

In the system (11) the force corresponding to the rotation Δφ is assumed to be the moment: $M = F_t.r$ and r is the first coordinate of node in cylindrical system in the final configuration.

$\boldsymbol{U}_k^i = <\ldots \ \Delta\varphi_k^i \ \ W_k^i \ \ldots>$, where i is the iteration and k is the number of node.

After transformation of displacements to the Cartesian coordinate using Equation (12), the initial positions can be updated to start a new iteration.

$$\begin{cases} U_p^i = U_r \cos\varphi - R_0(\ \cos(\varphi - \Delta\varphi^i) - \cos\varphi) \\ V_p^i = U_r \sin\varphi + R_0(-\sin(\varphi - \Delta\varphi^i) + \ \sin\varphi) \end{cases} \tag{12}$$

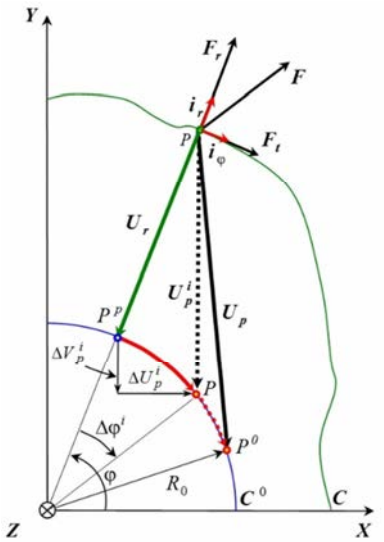

Fig. 2. Positions of point p in the initial configuration during iterations.

3. Application: Hydroforming of a T and Y-shaped tube

In this section, hydroforming modeling of a T and Y-shaped tubes is presented to show the efficiency of the IA for the tube hydroforming process using the simple initial geometric solution. The results of the IA are compared to those obtained by EDIA by ABAQUS® commercial code.

3.1. Application data

T and Y-shaped parts are among the cases where more of material feeding (in the circumferential direction of the tube in expansion zone) is necessary to carry out the part. This kind of tests has been studied by several authors experimentally and numerically using incremental codes but based on our knowledge they never used simplified approaches. The essential objective of this application is to demonstrate the effectiveness of our choice of initial solution to avoid the problem of vertical walls existing in the case of T-shaped tube and reverse taper presented in the case of Y-shaped tube.

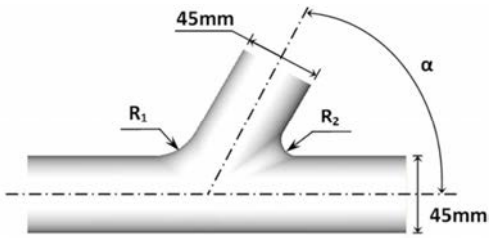

Fig. 3. The die geometry in the investigated process.

In this test a cylindrical low carbon steel (LCS 1008) tube of 45 mm (outer diameter), and 2 mm thickness was used as billet tube for both branches. A power law plasticity model $\overline{\sigma} = 722(0.041 + \overline{\varepsilon})^{0.52}$ which obtained from bulge test [9] was used for the simulation and the other material properties as: Young's modulus of 200 GPa, Poisson's ratio of 0.3 and density of 7800 kg/m^3.

The T and Y-models and their measurements are shown in Fig. 3 and table 1 with the process parameters. By taking advantage of symmetry, 1/2th of the Y-branch and 1/4th of the T-branch were modeled. To compare the two approaches, the final mesh obtained by ABAQUS® is taken for the IA modeling, containing 2091 nodes and 4000 3D shell elements. The tools are supposed rigid and modeled by discrete rigid shell and the interface between the tube and the die was modeled with an automatic surface-to-surface contact algorithm for the case of incremental method.

The evolutions of the normalized pressure and feeding (stroke) are given from the work of (Chebbah et.al [11]). The curves of the pressure and feeding in function of time allow controlling the strain path, leading to a fully formed tube without bursting.

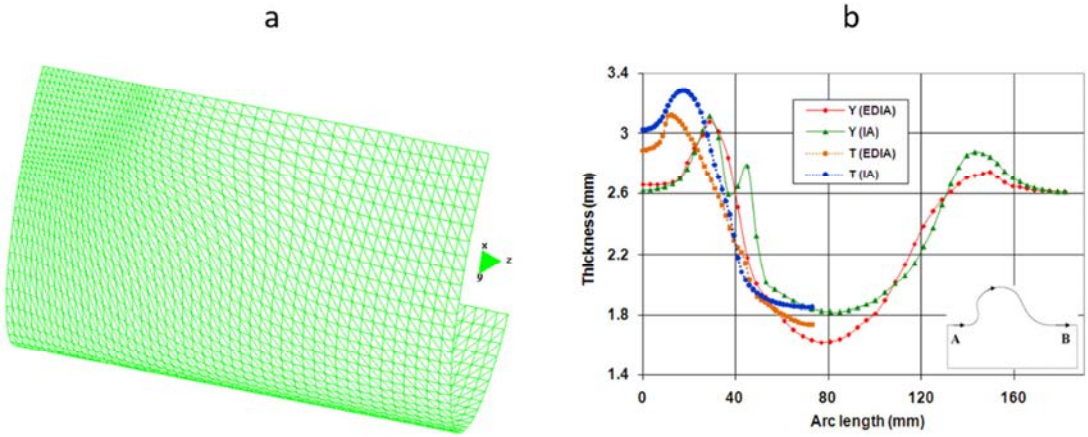

Fig. 4. (a) Initial guessed solution for T-shaped tube; (b) Thickness distribution along the line AB.

3.2. Numerical results

In this section we will present the simulation results of final tube wall thickness distribution for free T and Y-branch forming. The results of IA are compared with the results of EDIA of ABAQUS commercial code. During application, the relative displacement norm criteria and the relative residual norm criteria have been used with a tolerance of 10^{-6} [7].

Table 1. Geometry of the branches andprocess parameters.

Parameters	T-branch	Y-branch
Angle,α (°)	90	60
Right radius, R_1	18	30
Left radius, R_2	18	10
Final tube length, L (mm)	100	140
Right side stroke (mm)	34.56	25
Left side stroke (mm)	-34.56	-45
Maximum pressure, P_{max} (MPa)	44	50

Fig. 4(a) shows the initial guessed solution for the T-shaped tube obtained by a simple projection onto the intersection of the two axes of the branch (Fig. 1(a) and 3). This way of projection allows avoiding the superposition of nodes or the reversal of elements in the initial configuration.

To reduce the simulation time in incremental method case, the forming time used in the simulation was sped up by a factor of 1000 with apparently no ill effect for all our applications cases (see also Chebbah¸ et al. [7]). The branch height is obtained from the incremental simulation. This later reaches the maximum of 59.96 mm for Y-branch and 60.64 mm for T-branch at the end of process.

Table 2. Comparison of thicknessvariations.

		CPU times (s)	h_{min} (mm)	h_{max} (mm)
T-branch	IA	9.15	1.85	3.15
	EDIA	935	1.74	3.28
Y-branch	IA	9.78	1.81	3.11
	EDIA	661	1.61	3.08

In Fig. 5 we present the comparison between spectral thickness distributions obtained by the two methods (IA and EDIA) for the case of Y-branch. These results show a good agreement especially in the tip of the branch where the maximum of thinning is located. The minimum of thickness obtained is 1.82 mm with a relative error of 12.34% compared to the value obtained by EDIA using the ABAQUS code. The maximum thickening is remarked under the right entry radius of the Die, this maximum is 3.11mm with the IA and 3.08 mm with EDIA.

Also, Fig. 4(b) shows the thickness variation along the meridian profile (Arc A-B) for the two cases of T and Y-branch tubes. We can observe a good agreement between the two solutions. More quantitatively summary of thinning results and the CPU time for both two approaches are given in Table 2.

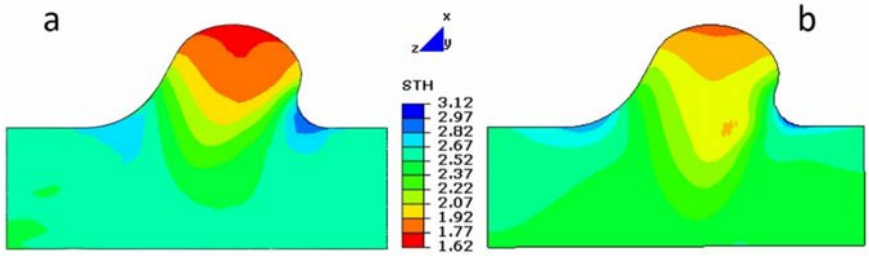

Fig. 5. Y-branch thickness distribution: (a) EDIA; (b) IA.

4. Conclusion

Simulation of anisotropic tube hydroforming operation using an inverse finite element approach has been presented in this paper. We have proposed a geometrical initial solution allows avoiding the problem of vertical walls and reverse taper. Numerical applications of tube hydroforming of T and Y-shaped tube, using the flow stress data obtained from bulge test have been utilized to validate the method. Verifications of the obtained results have been carried out using the classical EDIA by ABAQUS® commercial code. The results of numerical applications obtained encourage us to develop or adapt a general method for searching initial solution which makes our model capable to study more complicated parts.

References

[1] GuoYQ, Yuming Li, Boussad Abbès, Hakim Naceur and Ali Halouani, Damage Prediction in Metal Forming Process Modeling and Optimization Simplified Approaches, Handbook of Damage Mechanics, (2013) 1-43.
[2] GuoYQ, Batoz JL, Detraux JM, Duroux P. Finite element procedures for strain estimations ofsheet metal forming parts. Int. J. Numer. Method Eng. 30, 1385–1401 (1990).
[3] Liu SD, Karima M. A one step finite element approach for production design of sheet metal stamping, in: J.L. Chenot, R.D. Wood, O.C. Zienkiewicz(Eds.), NUMIFORM 92, Valbonne, France, A.A. Balkema, Rotterdam, 1992, p. 497.
[4] Nguyen BN, Johnson KI, Khaleel MA. Analysis of tube free hydroformingusing an inverse approach with FLD-based adjustment of process parameters.Journal of Manufacturing Science and Engineering 2003; 125:135–140.
[5] Fu L, Dong X, Wang P. Study on one-step simulation for the bending processof extruded profiles. International Journal of Advanced Manufacturing Technology 2009; 43 (11–12): 1069–1080.
[6] Chebbah MS, Naceur H, Hecini M. Rapid coupling optimization methodfor tube hydroforming process. Journal of Engineering Manufacture 2010. 224 (2), 245–256.
[7] Chebbah MS, Naceur Hand Gakwaya A. A fast algorithm for strain prediction in tube hydroforming based on one-step inverse approach. J Mater Process Technol. 211 (2011) 1898- 1906.
[8] Einolghozati M, Shirin MB, Assempour A. Application of inverse finite element method in tube hydroforming modeling. Applied Mathematical Modelling. 37 (2013) 5913–5926.
[9] Strano M, Altan T. “An inverse energy approach to determine the flow stress oftubular materials for hydroforming applications”. Journal of Materials Processing Technology 146 (2004) 92–96.
[10] Batoz JL, Dhatt G. Modélisation des structures par éléments finis1992, vol. 3. Editions Hermès, Paris, pp. 387–393 (in French).
[11] Chebbah MS, Azaouzi M. Geometrical Parameters Optimization for Tube Hydroforming using Response Surface Method, International Conference of Computational Methods in Sciences and Engineering, (ICCMSE), 04-07 April 2014, Athens, Greece.
[12] Abaqus Manual, Version 6.11. Dassault systems. May 2011, <http:// www.simulia.com>.